Cell Biochemistry and Biophysics (2022) 80:89–95
https://doi.org/10.1007/s12013-021-01025-5

ORIGINAL PAPER

INitial Steps of Insulin Action in Parotid Glands of Male Wistar Rats

André Guaraci DeVito-Moraes[1,2,3] · Victor Di Donato Marques[1] · Luciana Chagas Caperuto[1,4] · Flavia Kazue Ibuki[2] · Fernando Neves Nogueira[2] · Carlos Eduardo Francci[2] · Carla Roberta de Oliveira Carvalho[1]

Received: 13 July 2020 / Accepted: 14 July 2021 / Published online: 3 August 2021

Abstract

The parotid gland is the largest salivary gland. It produces watery saliva, rich in proteins (amylase, lysozymes, and antibodies). Due to the gland's morphological cytoarchitecture composed of only serous acini, it contributes almost 50% of total salivary volume upon stimulation. It has been reported that the prevalence of saliva secretion impairments, periodontitis, delayed wound healing, and xerostomia increase in diabetic patients. Herein we evaluated the acute effects of insulin on insulin receptor phosphorylation status and its substrates IRS-1 and IRS-2 in the parotid glands of adult male Wistar rats, using Western blot analyses. We confirmed an acute effect of insulin on IR/IRS/PI3K/Akt and MAPK intracellular pathway activation in the parotid glands of male Wistar rats similar to the classical metabolic targets of the hormone, like the liver.

Keywords Parotid Gland · Insulin · Intracellular Signaling, Rats.

Introduction

Insulin is a protein hormone produced and secreted by the pancreatic β-cells mainly in response to elevated blood glucose levels. Its actions involve modulating tissue targets by binding to the transmembrane insulin receptor (IR) and subsequent promotion of the tyrosine kinase activity of its receptor [1, 2]. It is well established that the initial intracellular insulin signaling pathway targets tissues associated with metabolic homeostasis, such as the liver, adipose tissue, and skeletal muscle [3–6].

The IR is a heterotetrameric transmembrane glycoprotein with intrinsic protein tyrosine kinase activity, composed of two α and two β-subunits [7, 8]. The α-subunits are completely extracellular and contain the insulin-binding domain, whereas the β-subunits contain an extracellular domain, a transmembrane domain and an intracellular tail [9, 10]. The intracellular domain contains a Tyr-specific protein kinase that is immediately activated after insulin binding, initiating a cascade of autophosphorylation events within the β-subunits and leading to the phosphorylation of its substrates, namely IRS-1 and IRS-2 [11–13]. The phosphorylation of these substrates is linked to the activation of two main signaling pathways, the phosphatidylinositol 3-kinase (PI3K)-AKT/protein kinase B (PKB) and the ras-mitogen-activated protein kinase (MAPK) [14–21]. Once activated, MAPK stimulates serine-kinase proteins, including the ERKs, which ultimately catalyze transcription factors, inducing cellular differentiation and proliferation [22].

Several studies have shown that individuals with type 2 diabetes mellitus (T2DM) present differences in the salivary parameters, including total salivary protein and ion concentrations [23–26]. In diabetic rats, it was reported that the volume, flow rate, and protein secretion rate of saliva were reduced after acid stimulation, especially in the parotid gland [27].

Despite the parotid gland being the largest salivary gland and only containing serous cells, the most studied salivary gland is the submandibular gland. Indeed, streptozotocin diabetes mellitus (STZ-DM) rats or physiological aged rats present modifications in the intracellular insulin signaling pathway in the submandibular salivary

✉ André Guaraci DeVito-Moraes
adevito@alumni.usp.br

1 Department of Physiology and Biophysics, Institute of Biomedical Sciences, University of São Paulo (USP), Av. Prof. Lineu Prestes, 1524, São Paulo, SP 05508-000, Brazil

2 Department of Biomaterials and Oral Biology, School of Dentistry, University of São Paulo (USP), Av. Prof. Lineu Prestes, 2227, São Paulo, SP 05508-000, Brazil

3 Discipline of Dental Biomaterials, School of Dentistry, University Nove de Julho (UNINOVE), Rua Vergueiro, 235/249, São Paulo, SP 01504-001, Brazil

4 Department of Biological Sciences, Federal University of São Paulo (UNIFESP), R. Prof. Artur Riedel, 275, Diadema, SP 09972-270, Brazil

glands [28, 29]. However, while the submandibular and sublingual glands support basal saliva secretion, the parotid gland produces ~50% of the saliva upon stimulation. Moreover, the acinar serous produces and secretes amylase and other proteins, including immunoglobulin, lactoperoxidase, melanotransferrin, and deoxyribonuclease [30]. Previous studies have shown that the principal regulatory mechanism of salivary gland production and secretion involves the autonomous nervous system [30, 31]. In this sense, the sympathetic branch regulates the secretion of the saliva proteins and the parasympathetic nerve regulates the saliva secretion. Interestingly, the potential use of glucose and amylase in saliva has been proposed as a diagnostic tool for the early detection of T2DM [32–34].

In diabetic animals, the proposed mechanism involves a dysfunctional autonomic nerve system [35, 27], inflammatory cellular infiltration and oxidative stress [27] in the salivary glands. However, the potential effect of insulin on the parotid gland cannot be ruled out. Thus, in the present study, we analyzed the intracellular insulin signaling pathway in the parotid gland of male adult rats and observed an activation pattern of the IR/IRS/PI3K/AKT/MAPK pathway similar to classical insulin signaling in other insulin targeted tissues.

Materials and Methods

Reagents

The reagents and apparatus for SDS-PAGE and Western blotting procedures were from Bio-Rad (Richmond, CA, USA). The chemicals Tris, phenylmethylsulfonylfluoride (PMSF), aprotinin and dithiothreitol were from Sigma-Aldrich (St Louis, MO, USA). Sodium thiopental was from Cristália (Itapira, SP, Brazil). Human recombinant insulin (Humulin R) was purchased from Eli Lilly Co. (Indianapolis, IN, USA). Anti-IR, anti-IRS-1, anti-IRS-2, anti-phosphotyrosine and anti-SHP2 antibodies came from Santa Cruz Biotechnology (Santa Cruz, CA, USA). The anti-PI3-kinase (p85 subunit) antibody was from Upstate Biotechnology (Lake Place, NY, USA). Phospho-AKT (Ser^{473}) and phospho-ERK1/2 (Thr^{202}/Tyr^{204}) antibodies were from New England Bio Labs (Beverly, MA, USA). The enhanced chemiluminescence (ECL) reagent kit and the protein A-Sepharose 6 MB were from Amersham-Pharmacia Biotech (Buckinghamshire, UK).

Animals

Fifty-four male Wistar rats (250–300 g), 8–12 weeks old, were employed for the present study. The animals were provided with standard rodent chow and tap water *ad libitum*. They were housed in a temperature-controlled room at 25 °C with a 12/12-hour dark and light cycle. Before the experiment, the animals fasted for 12–14 h. All the procedures involving animal experimentation were conducted in strict accordance with Brazilian legislation (N°. 11794) and the Ethics Committee on the Use of Animals at ICB-USP.

Methods

The rats were deeply anesthetized with sodium thiopental (50 mg/kg body weight). Under basal conditions, we extracted rat bilateral parotid glands before or 3, 5, and 10 min after administering 6 µg of insulin through the portal vein. Liver fragments were also extracted 30 s after insulin infusion, representing a positive control for insulin intracellular pathway activation under basal conditions [4]. The samples were then processed and insulin-induced tyrosine phosphorylation of the insulin receptor (IR) and the insulin receptor substrates (IRS-1 and IRS-2) was evaluated using Western blot analysis.

Another set of anesthetized rats was infused with 0.5 mL of a saline solution (0.9% NaCl) with or without 0.03 ng, 0.3 ng, 3 ng, 0.03 µg, and 0.3 µg of insulin. The data from this set of experiments was used to determine the dose-dependent effects of insulin.

The relative abundance of IR, IRS-1 and IRS-2 was assessed by first removing the parotid gland, adding 200 µl of ice-cold homogenization buffer (100 mM Tris, pH 7.6, 1% Triton X-100, 0.01 mg/ml aprotinin, 2 mM PMSF, 10 mM Na_3VO_4, 10 mM NaF, 10 mM $Na_4P_2O_7$, and 10 mM EDTA), and homogenizing the sample in a Polytron PTA 2100 for 30 s. Insoluble material was removed by centrifugation for 30 min at 30,000 × *g* in a Beckman 70.1 Ti rotor (Palo Alto, CA, USA) at 4 °C. Aliquots of the isolated supernatants represent the whole tissue extract of the samples, which were loaded onto SDS-PAGE gels and subjected to SDS-PAGE. In addition, 150 µg of total protein was removed from each whole tissue sample and immunoprecipitated with 10 µl (0.2 µg/ml) of anti-IR, anti-IRS-1 or anti-IRS-2 antibodies. Target-bound antibodies were recovered using protein A-Sepharose 6MB, and the samples were resolved by SDS-PAGE electrophoresis. The SDS-PAGE procedure employed for separating the whole tissue extract and immunoprecipitated proteins involved adding Laemmli sample buffer [36] containing 100 mM DTT, loading the samples onto 6.5% or 8% gels and running the gels in a miniature lab gel apparatus.

The gel proteins were transferred to nitrocellulose membrane by applying 120 V for 90 membranes in a Bio-Rad transfer apparatus. The nitrocellulose membranes were incubated overnight at 4 °C in blocking buffer (5% non-fat dry milk, 10 mM Tris, 150 mM NaCl and 0.02% Tween 20)

to reduce non-specific protein binding. Then the membranes were incubated at 22 °C for four hours with primary antibodies against anti-phosphotyrosine, anti-p85 PI3K, anti-SHP2, anti-pSer AKT, and anti-pMAPK diluted, as indicated by the manufacturer, in blocking buffer with 3% non-fat dry milk. Next, the membranes were washed, and the appropriate secondary antibodies were applied at dilutions recommended by the manufacturer. Finally, the immunoblots were washed, developed using ECL and exposed to radiographic film.

Data Analysis

The results are presented as the mean ± standard deviation (SD) of arbitrary units (AU). Band intensities were quantified using the Image J software (https://imagej.nih.gov). Statistical analyses included one-way ANOVA and Tukey's post-test of multiple comparisons using the GraphPad Prism version 9.1.0 software. The level of statistical significance was set at $p < 0.05$.

Results

Dose-response of Insulin Receptor β-subunit and pp185 Tyrosyl Phosphorylation in the Parotid Gland

As shown in Fig. 1A, an acute insulin infusion increased phosphorylated tyrosine levels in the whole gland tissue extract in a time-dependent manner. Notably, a similar response was also detected in liver samples, the classical insulin tissue target (i.e., positive control), collected 30 s after the infusion. Upon closer examination, under basal conditions, at time point 0, there are three faint bands in the parotid gland and liver samples. Following the insulin infusion, increased intensity of two bands was observed in both tissues. Based on the apparent molecular weights, the upper band, denoted pp185, contains both IRS-1 and IRS-2, while the lower band, migrating at an estimated molecular weight of 75–100 kDa, corresponds to the IR β-subunit. Evaluating the time dependence of the enhanced phosphorylation indicated that maximal insulin-induced tyrosine phosphorylation in the parotid glands occurred 5 min after the infusion.

In Fig. 1B, we investigated the effect of insulin dose on IR phosphorylation. There was a detectable dose-dependent increase in IR phosphorylation in samples treated with insulin and immunoprecipitated with an anti-IR antibody. Moreover, the lowest insulin dose required to elicit this enhanced tyrosine phosphorylation response was found to be on the order of 3.10^{-4} ug. Samples treated with 10^{-1} ug insulin, a concentration close to physiological postprandial values, displayed intense phosphorylated IR bands.

THe Initial Steps of Insulin Action are Activated in Parotid Glands

Next, we immunoprecipitated the whole tissue samples collected 3, 5 and 10 min after insulin infusion with antibodies against IR (Fig. 2A), IRS-1 (Fig. 2B) and IRS-2 (Fig. 2C). Interestingly, we observed a significant 5- to 7-fold-increase ($p < 0.05$) in insulin-induced IR tyrosine phosphorylation at all three times analyzed (Fig. 2A). There was also a significant increase in insulin-induced IRS-1

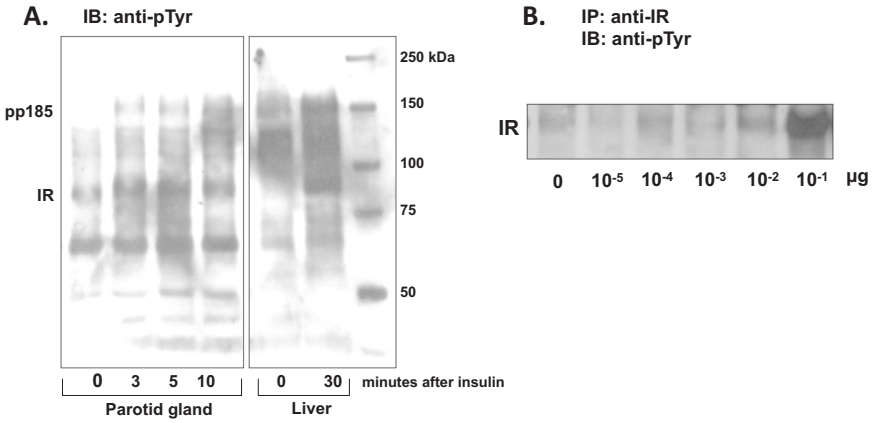

Fig. 1 Time-course (**A**) and dose-dependent effect (**B**) of insulin-induced tyrosyl phosphorylation during the initial steps of the intracellular insulin signaling pathway. Parotid glands were extracted from anesthetized overnight fasted rats as described in the Methods section. The time-course effect was analyzed using whole tissue extract, and the proteins were separated on 6% SDS-PAGE gels, followed by Western blot analysis with anti-phosphotyrosine antibody (anti-pTyr). The dose-dependent effect was evaluated in samples that were immunoprecipitated using an antibody against the β-subunit of the insulin receptor (anti-IR). The antibody was diluted following the manufacturer's instructions. The immunoblot results are representative of three distinct experiments. Each lane corresponds to a sample from one animal ($n = 30$)

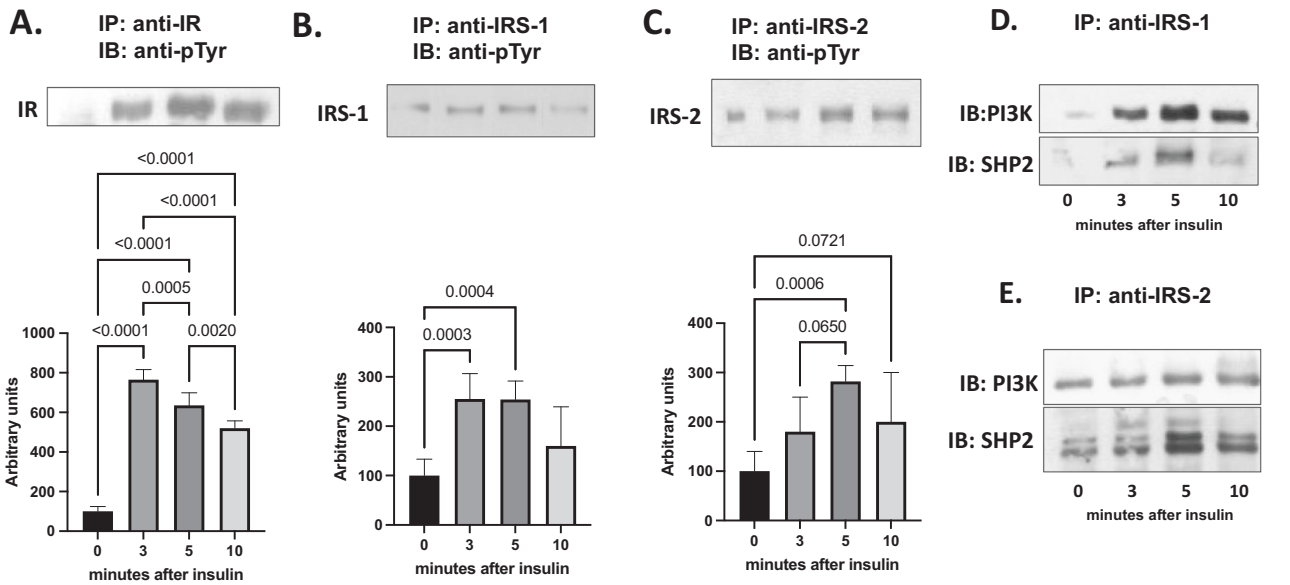

Fig. 2 Monitoring the initial steps of the intracellular insulin signaling pathway in the parotid gland. Parotid glands were extracted from anesthetized overnight fasted rats as described in the Methods section. Insulin-induced tyrosyl phosphorylation of the IR (**A**), IRS-1 (**B**) and IRS-2 (**C**), the insulin-induced association of IRS-1 with the p85 subunit of PI3K or SHP2 (**D**), and the insulin-induced association of IRS-2 with the p85 subunit of PI3K or SHP2 (**E**). The antibodies were diluted following the manufacturer's instructions. The data in the graphs are presented as the mean ± SD of six experiments. One-way ANOVA and Tukey's post-test of multiple comparisons were used to compare samples. Results with p values less than or equal to when 0.07 are displayed. We utilized samples from 24 rats for the data presented in this figure

tyrosine phosphorylation, which approached a 2.5-fold increase three and 5 min after hormone injection. However, after 10 min, phosphorylated IRS-1 levels were attenuated to levels that were not statistically different from control levels. Immunoprecipitating the samples with an antibody against IRS-2 revealed significant insulin-induced tyrosine phosphorylation of this protein five and 10 min after insulin infusion. The results confirm insulin-induced activation of the intracellular insulin pathway in the parotid glands.

The subsequent step in the intracellular insulin pathway involves the insulin-induced association of IRS-1 and IRS-2 with the kinase PI3K and the phosphatase SHP2. Therefore, we immunoprecipitated samples collected 0-10 after insulin injection with an antibody against IRS-1 and IRS-2 and then probed the isolated products using anti-PI3K and anti-SHP2 antibodies (Fig. 2D, E). These results illustrate the association between IRS-1/p85-PI3K, IRS-1/SHP2, IRS-2/p85-PI3K, and IRS-2/SHP2. We observed a similar relationship between insulin-induced IRS-1 tyrosine phosphorylation and its association with the downstream PI3K and SHP2 proteins (Fig. 2D). In contrast, while a relationship appears to exist between IRS-2 tyrosine phosphorylation and its association with SHP2, this was not observed with PI3K (Fig. 2E). These results provide further evidence of intracellular insulin signaling in the parotid gland.

Finally, we analyzed the downstream intracellular pathways involving the PI3K/AKT and the MAPK in the parotid gland. A twofold increase in AKT serine phosphorylation levels was detected 3 min after insulin infusion, and these levels remained significantly elevated until the ten-minute time point (Fig. 3A). A similar pattern was also observed with the phosphorylation status of MAPK, also known as ERK1 and ERK2, in which there was a sustained ~3-fold increase for 10 min after insulin infusion (Fig. 3B).

Discussion

We detected insulin-induced IR tyrosine phosphorylation in the parotid glands of healthy adult rats in the present study. Insulin also induced IRS-1 and IRS-2 tyrosine phosphorylation at the physiological insulin blood concentration [11–13]. Notably, the IRS-1/2 proteins are essential for insulin signaling, activating several enzymes [2] to ensure insulin's pleiotropic effects. It is also important to point out that, like in the liver, insulin-induced IR, IRS-1, and IRS-2 tyrosine phosphorylation occurs in a time-dependent fashion in the parotid gland. Furthermore, it was found that insulin could influence the association between IRS1/2 with and SHP2 and/or PI3K [14] and AKT and MAPK phosphorylation. Indeed, previous work in classical insulin targeted tissues revealed that proteins such as SHP2, Nck, GRB-2, and p85 subunit of the PI3K, which have the SH2 domain associate with phosphorylated IRS-1/2 [2].

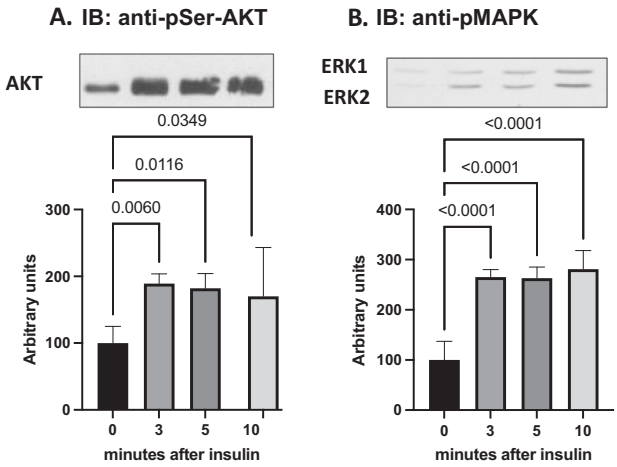

Fig. 3 Insulin-induced Akt serine phosphorylation (**A**) and MAPK phosphorylation (**B**) in the parotid gland. Parotid glands were extracted from anesthetized overnight fasted rats as described in "Methods" section. The antibodies were diluted following the manufacturer's instructions. The data in the graphs are presented as the mean ± SD of similar experiments. The data in the graphs are presented as the mean ± SD of six experiments. One-way ANOVA and Tukey's post-test of multiple comparisons were used to compare samples. Results with p values less than or equal to when 0.06 are displayed. We utilized samples from 24 rats for the data presented in this figure

It has been reported that SHP2 is a phosphotyrosine phosphatase with two SH2 domains [12]. Interestingly, this phosphatase has been implicated as a positive regulator of insulin signaling [37], participating in various signal transduction processes, including the Ras-Raf-MaAP kinase, PI3 kinase, and Jak-Stat pathways [22]. Moreover, the IRS-1/PI3-K association has been implicated in glucose transport [38, 39], glycogen synthesis, gluconeogenesis via phosphoenol-pyruvate carboxykinase inhibition [2, 40], and cellular growth [39] in most tissues studied. There is also evidence that AKT activation can overwhelm apoptosis induced by different stimuli [41]. In this regard, some of these biological effects could be occurring in the parotid gland. Therefore, identifying the classic intracellular cascade of insulin action in the parotid glands reveals essential information for gland physiology and amplifies our understanding of endocrine regulation [32–34].

Our results are clinically relevant since it is well known that individuals with T1DM and T2DM sometimes experience salivary flux reduction and xerostomia [42, 43]. In this sense, an insulin resistance status increases salivary Ca^{2+} concentrations and reduces Mg^{2+}, Zn^{2+}, and K^{+} concentration, which has been associated with attenuated salivary flow rate, increased oral infection occurrence, and periodontitis development [44–46].

Although the principal mechanism of salivary flux involves the autonomous nervous system, identifying the initial steps of the insulin pathway in the parotid gland opens the possibility of understanding the potential action of this hormone in the salivary flux and amylase production and secretion. The relatively specific anatomical identification of islets of adipose cells in the parotid gland compared to other salivary glands [47] is particularly interesting and requires additional functional and molecular studies focused on insulin signaling in the salivary glands.

Conclusion

The rat parotid gland exhibits all the initial steps of the insulin signaling pathway and appears to respond in a manner like the liver, a classical insulin-targeted tissue. These data open up the possibility for further research into parotid gland insulin regulation, function and metabolism.

Compliance with Ethical Standards

Conflict of Interest The authors declare no competing interests.

Publisher's note Springer Nature remains neutral with regard to jurisdictional claims in published maps and institutional affiliations.

References

1. White, M. F., Shoelson, S. E., Keutmann, H., & Kahn, C. R. (1988). A cascade of tyrosine autophosphorylation in the beta-subunit activates the phosphotransferase of the insulin receptor. *Journal of Biological Chemistry*, *263*(6), 2969–2980.
2. Cheatham, B., & Kahn, C. R. (1995). Insulin action and the insulin-signaling network. *Endocrine Review*, *16*, 117–142.
3. Cuatrecasas, P. (1969). Interaction of insulin with the cell membrane: the primary action of insulin. *Biochem*, *63*, 450–457.
4. Cuatrecasas, P. (1972). Affinity chromatography and purification of the insulin receptor of liver cell membranes. *Proceedings of the National Academy of Sciences of the United States of America*, *69*, 1277–1281.
5. Freychet, P., Roth, J., & Neville, D. M. (1971). Monoiodoinsulin: demonstration of its biological activity and binding to fat cells and

liver membranes. *Biochemical and Biophysical Research Communications*, *43*(2), 400–408.
6. Freychet, P., Roth, J., & Neville, D. M. (1971). Insulin receptor in the liver: specific bindidng of [125I] insulin to the plasma membrane and its relation to insulin bioactivity. *Proceedings of the National Academy of Sciences of the United States of America*, *68*, 1833–1837.
7. Kahn, C. R. (1985). Molecular mechanism of insulin action. *Annual Review of Medicine*, *36*, 429–451.
8. Patti, M. E., & Kahn, C. R. (1998). The insulin receptor—a critical link in glucose homeostasis and insulin action. *Journal of Basic and Clinical Physiology and Pharmacology*, *9*, 89–109.
9. Kasuga, M., Karlsson, F. A., & Kahn, C. R. (1982). Insulin stimulates the phosphorilation of the 95.000 dalton subunit of its own receptor. *Science*, *215*, 185–187.
10. Ullrich, A., & Schlessinger, J. (1990). Signal transduction by receptors with tyrosine kinase activity. *Cell*, *61*(2), 203–212.
11. Cahill, G., & FJr (1971). Phisiology of insulin in man. *Diabetes*, *20*, 785–799.
12. Sun, X. J., Rothenberg, P., Kahn, C. R., Backer, J. M., Araki, E., Wilden, P. A., Cahill, D. A., Goldstein, B. J., & White, M. F. (1991). Structure of the insulin receptor substrate IRS-1 defines a unique signal Transduction protein. *Nature*, *352*, 73–77.
13. Sun, X. J., Wang, L. M., & Zhang, Y., et al. (1995). The structure and function of 4PS reveals IRS-2: A common interface in insulin and cytokine signaling. *Nature*, *374*, 442–446.
14. Folli, F., Saad, M. J. A., Backer, J. M., & Kahn, C. R. (1992). Insulin stimulation of phosphatidylinositol 3-kinase and association with insulin receptor substrate 1 in liver and muscle of the intact rat. *Journal of Biological Chemistry*, *267*, 22171–22177.
15. Kohn, A. D., Summers, S. A., Birnbaum, M. J., Roth, R. A. (1996). Expression of a constitutively active AKT Ser/Thr Kinase in 3T3-L1 adipocytes stimulates glucose uptake and glucose transporter 4 translocation. *Journal of Biological Chemistry*, 6:271 (49), 31372–31378.
16. Tanti, J. F., Grillo, S., Gremeaux, T., Coffer, P. J., Van Ibberghen, E., & Le Marchand-Brustel, Y. (1997). Potential role of protein Kinase B in glucose transporter 4 translocation in adipocytes. *Endocrinology*, *138*(5), 2005–2010.
17. Krook, A., Roth, R. A., Jiang, X. J., Zierath, J. R., & Wallberg-Henriksson, H. (1998). Insulin-stimulated AKT Kinase activity is reduced in skeletal muscle from NIDDM subjects. *Diabetes*, *47* (8), 1281–1286.
18. Shepherd, P. R., Nave, B. T., & Siddle, K. (1995). Insulin stimulation of glycogen synthesis and glycogen synthase activity is blocked by wortmannin and rapamycin in 3t3-L1 adipocytes: evidence for the involvement of phosphoinositide 3-Kinase and p70 ribosomal protein-S6 kinase. *Journal of Biological Chemistry*, *305*, 25–28.
19. Kovacina, K. S., & Roth, R. A. (1993). Identification of shc as a substrate of the insulin receptor Kinase distinct from the GAP-associated 62 kDa tyrosine phosphoprotein. *Biochemical and Biophysical Research Communications*, *192*, 1303–1311.
20. Wang, L. M., Myers, M. G., Sun, X., Aaronson, S. A., White, M., & Pierce, J. H. (1993). IRS-1: Essential for insulin and IL-4 stimulated mitogenesis in hematopoietic cells. *Science*, *261*, 1591–1594.
21. Avruch, J. (1998). Insulin signal transduction through protein kinase cascades. *Molecular and Cellular Biochemistry*, *182*(1-2), 31–48.
22. Boulton, T. G., Nye, S. H., Robbins, D. J., Ip, N. Y., Radziejewska, E., Morgenbesser, S. D., DePinho, R. A., Panayotatos, N., Cobb, M. H., & Yancopoulos, G. D. (1991). ERKs a family of protein-serine/threonine kinases that are activated and tyrosine phosphorylated in response to insulin and NGF. *Cell*, *65*, 663–675.
23. Bakianian-Vaziri, P., Vahedi, M., Mortazavi, H., Abdollahzadeh, S. H., & Hajilooi, M. (2010). Evaluation of salivary glucose, IgA and flow rate in diabetic patients: a case-control study. *Journal of Dental Medicine - Tehran*, *7*, 13–18.
24. Indira, M., Chandrashekar, P., Kattappagari, K. K., Chandra, L. P., Chitturi, R. T., & BV, R. R. (2015). Evaluation of salivary glucose, amylase, and total protein in type 2 diabetes mellitus patients. *Indian Journal of Dental Research*, *26*, 271–275.
25. Panchbhai, A. S., Degwekar, S. S., & Bhowte, R. R. (2010). Estimation of salivary glucose, salivary amylase, salivary total protein and salivary flow rate in diabetics in India. *Journal of Oral Science*, *52*, 359–368.
26. Marín Martínez, L., Molino Pagán, D., & López Jornet, P. (2018). Trace elements in saliva as markers of type 2 diabetes mellitus. *Biological Trace Element Research*, *186*, 354–360.
27. Chen, S. Y., Wang, Y., Zhang, C. L., & Yang, Z. M. (2020). Decreased basal and stimulated salivary parameters by histopathological lesions and secretory dysfunction of parotid and submandibular glands in rats with type 2 diabetes. *Experimental and Therapeutic Medicine*, *19*(4), 2707–2719.
28. Rocha, E. M., Lima, M. H. M., Carvalho, C. R. O., Saad, M. J. A., & Velloso, L. A. (2000). Characterization of the insulin-signaling pathway in lacrimal and salivary glands of rats. *Current Eye Research*, *21*(5), 833–842.
29. Rocha, E. M., Carvalho, C. R. O., Saad, M. A. J., & Velloso, L. A. (2003). The influence of ageing on the insulin signalling system in rat lacrimal and salivary glands. *Acta Ophthalmologica Scandinavica*, *81*(6), 639–645.
30. Young, J. A., Van Lennep, D. W. (1978). The morphology of salivary glands. London, New York, Academic Press.
31. Mason, D. K., Chisholm, D. M. (1975). Salivary glands in health and disease. London, Philadelphia, Saunders.
32. Mascarenhas, P., Fatela, B., & Barahona, I. (2014). Effect of diabetes mellitus type 2 on salivary glucose-a systematic review and meta-analysis of observational studies. *Plos One*, *9*(7), e101706.
33. Naseri, R., Mozaffari, H. R., Ramezani, M., & Sadeghi, M. (2018). Effect of diabetes mellitus type 2 on salivary glucose, immunoglobulin A, total protein, and amylase levels in adults: a systematic review and meta-analysis of case-control studies. *Journal of Research in Medical Sciences*, *23*, 89
34. Pérez-Ros, P., Navarro-Flores, E., Julián-Rochina, I., Martínez-Arnau, F. M., & Cauli, O. (2021). Changes in salivary amylase and glucose in diabetes: a scoping review. *Diagnostics*, *11*(3), 453.
35. Anderson, L. C., Garrett, J. R., Thulin, A., & Proctor, G. B. (1989). Effects of streptozocin-induced diabetes on sympathetic and parasym-pathetic stimulation of parotid salivary gland function in rats. *Diabetes*, *38*, 1381–1389.
36. Laemmli, U. K. (1970). Cleavage of structural proteins during the assembly of the head of bacteriophage T4. *Nature*, *227*, 680–685.
37. Copps, K. D., & White, M. F. (2012). Regulation of insulin sensitivity by serine/threonine phosphorylation of insulin receptor substrate proteins IRS1 and IRS2. *Diabetologia*, *55*, 2565–2582.
38. Clarke, J. F., Young, P. W., Yonezawa, K., Kasuga, M., & Holman, G. D. (1994). Inhibition of the Translocation of GLUT1 and GLUT4 in 3T3-L1 cells by the Phosphatidylinositol 3-Kinase inhibitor, wortmannin. *Biochem J*, *300*(Pt3), 631–635.
39. Tsakiridis, T., McDowell, H. E., Walker, T., Downes, C. P., Hundal, H. S., Vranic, M., & Klip, A. (1995). Multiple roles of phosphatidylinositol 3-kinase in regulation of glucose transport, amino acid transport, and glucose transporters in L6 skeletal muscle cells. *Endocrinology*, *136*(10), 4315–4322.
40. Sanches-Margalet, V., Goldfine, I. D., Vlahos, C. J., & Sung, C. K. (1994). Role of PI 3-kinase in insulin receptor signaling: studies with inhibitor LY294002. *Biochemical and Biophysical Research Communications*, *204*, 336–LY294452.

41. Limesand, K. H., Barzen, K. A., Quissel, D. O., & Anderson, S. M. (2003). Synergistic suppression of apoptosis in salivary acinar cells by IGF1 and EGF. *Cell Death and Differentiation*, *10*, 345–355.
42. Hoseini, A., Mirzapour, A., Bijani, A., & Shirzad, A. (2017). Salivary flow rate and xerostomia in patients with type I and II diabetes mellitus. *Electron Physician*, *9*(9), 5244–5249.
43. Newrick, P. G., Bowman, C., Green, D., O'Brien, I. A., Porter, S. R., Scully, C., & Corrall, R. J. (1991). Parotid salivary secretion in diabetic autonomic neuropathy. *Journal of Diabetic Complications*, *5* (1), 35–37.
44. Mata, A. D., Marques, D., Rocha, S., Francisco, H., Santos, C., Mesquita, M. F., & Singh, J. (2004). Effects of diabetes mellitus on salivary secretion and its composition in the human. *Molecular and Cellular Biochemistry*, *261*(1-2), 137–142.
45. Benguigui, C., Bongard, V., Ruidavets, J. B., Chamontin, B., Sixou, M., Ferrières, J., & Amar, J. (2010). Metabolic syndrome, insulin resistance, and periodontitis: a cross-sectional study in a middle-aged French population. *Journal of Clinical Periodontology*, *37*(7), 601–608.
46. Timonen, P., Suominen-Taipale, L., Jula, A., Niskanen, M., Knuuttila, M., & Ylöstalo, P. (2011). Insulin sensitivity and periodontal infection in a non-diabetic, non-smoking adult population. *Journal of Clinical Periodontology*, *38*(1), 17–24.
47. Tanakchi S., Aly F. Z. Anatomy & histology. PathologyOutlines.com, website. https://www.pathologyoutlines.com/topic/salivaryglandsnormalhistology.html.